



Nodular lymphocyte-predominant Hodgkin lymphoma and clinical impact of its variant histology: a clinicopathologic study from tertiary cancer centre in India

Nikita J. Mulchandani¹ · Ann Kurian¹ · Annapurneswari Subramanyan¹

Received: 6 April 2022 / Accepted: 2 August 2022 / Published online: 23 August 2022
© The Author(s), under exclusive licence to Springer-Verlag GmbH Germany, part of Springer Nature 2022

Abstract

Nodular lymphocyte-predominant Hodgkin lymphoma (NLPHL) can show variant histological patterns, some of which may be associated with an advanced stage and increased relapse rate. Through this study, we put the various histological patterns of NLPHL under spotlight and assess their prognostic implications. A retrospective histologic and immunohistochemistry review of all archival slides of NLPHL over a period of 6 years was performed. A total of 36 cases were identified. We recognised the typical (A, B) and histopathologic variant patterns (C to F) of NLPHL as per the criteria given by Fan et al. and scored these cases using the 5 histological parameters described by Shet et al. Complete clinical follow-up information could be obtained in 25 cases. Patients with NLPHL constituted 6.4% of Hodgkin lymphoma cases in our institute. While predominant typical histological patterns were seen in 9/36 patients, variant patterns C, D, E, and F were observed in 15, 3, 7, and 2 cases respectively. All cases with typical growth patterns showed a score of ≤ 5 and those with variant histologies showed scores between 2 and 9. Relapse of lymphoma was seen in 7 cases, all of which showed a variant histology. The histopathological scores increased or stayed constant at the time of relapse. Histopathological growth patterns at the time of initial diagnosis and disease relapse were consistent in 6/7 cases. Transformation to large B-cell lymphoma was seen in 1 case. We could conclude that NLPHL cases with variant histology showed an increased risk of relapse. The histopathological growth patterns remained consistent in majority cases at relapse.

Keywords Hodgkin lymphoma · NLPHL · Relapse · Prognostic · B-cell lymphoma

Introduction

Nodular lymphocyte-predominant Hodgkin lymphoma (NLPHL) is a unique and rare subtype of Hodgkin lymphoma (HL) which accounts for approximately 10% of all HL cases. NLPHL can occur in a wide age range affecting both children and older patients [1]. It is a potentially curable germinal centre (GC) B-cell malignancy with localised peripheral lymph node (LN) involvement, usually an indolent disease course with long-term remission rates of > 90% [2, 3]. Involvement of extranodal sites like liver, spleen, lungs and bone marrow is seen in advanced stage nodal disease [4].

NLPHL is characterised by nodular or nodular and diffuse proliferation of large lymphocyte-predominant (LP) or ‘popcorn’ cells with multilobated, folded nuclei in a background composed of variable number of reactive small B- and T-lymphocytes. Fan et al. in their pioneering article described six different immunomorphological patterns of NLPHL. These included typical (a) pattern A: ‘classic’ (B-cell-rich) nodular, (b) pattern B: serpiginous/interconnected nodular, variant (c) pattern C: nodular with prominent extra nodular LP cells, (d) pattern D: T-cell-rich nodular, (e) pattern E: diffuse with a T-cell-rich background (T-cell/histiocyte-rich large B-cell lymphoma [THRLBCL]-like), and (f) pattern F: (diffuse) B-cell rich [1, 5]. The histopathologic variants often show an aggressive disease course with multiple relapses [3, 6, 7].

To simplify the variable histologic descriptions of NLPHL, Shet et al. devised a 3-tier histologic scoring system based on quantification of 5 histological parameters (Table 1) serving as a guide to distinguish typical and variant

✉ Nikita J. Mulchandani
nikitamulchandani@gmail.com

¹ Department of Surgical Pathology, Apollo Cancer Centre, Chennai, India

Table 1 The histological scoring system by Shet et al. [8]

Parameter	Pattern grading	Score
Percentage of nodularity as seen on hematoxylin and eosin (H&E)-stained sections	Nodular throughout (100%)	0
	Mostly nodular with $\geq 75\%$ but $< 100\%$ nodularity	1
	Tumors with $< 75\%$ nodularity	2
Extranodular LP cells as seen on a CD20 stain	None to $< 15\%$ of the node showing extra nodular LP cells	0
	≥ 15 to $\leq 50\%$ extra nodular LP cells	1
	$> 50\%$ of node area showing extra nodular LP cells	2
Cell composition ratio of T-cells vs B-cells on CD3 and CD20 stains	B-cell-rich tumor with T-cell-rich area $< 20\%$	0
	T-cells moderately increased (T-cell area 21–50%)	1
	T-cell-rich tumors ($> 50\%$ T-cell areas)	2
Types of nodules as seen on H&E and CD20	Well-defined, uniformly distributed seen on H&E	0
	Irregular nodules, margins not defined, better seen on CD20	1
	Multinodular, interconnected seen on H&E	2
Loss of dendritic network on CD23 staining	Focally or completely preserved throughout the nodules	0
	Lost in most areas except for a few strands	1
Maximum score		10

patterns. They defined a ‘perfect’ nodule in NLPHL as well defined, purely showing B-cells with CD3-positive cells seen rosetting around the LP cells. An increase in T-cells in some cases of NLPHL leads to loss of dendritic network, resulting in breakdown of the B-cell-rich nodules and slipping out of the LP cells which are then perceived as extranodular LP cells. This concept formed the basis of their scoring system. After risk stratification, they concluded that while score < 6 was seen in typical NLPHL cases, tumors with scores > 6 showed a higher relapse potential. Therefore, the quantification of these histologic parameters helps oncologists understand the degree of variation in NLPHL and identify cases which demand an aggressive approach [8].

Typically, the LP cells do not show a down-regulation of B-cell programme and are characteristically positive for CD20, CD79a, PAX5, OCT2, and BOB.1 suggesting a preserved B-cell phenotype. They also show a retained CD45 expression. BCL6 positivity in LP cells points towards their GC origin. However, CD10 is negative. Also, as opposed to classical HL, these LP cells are usually CD30 negative and are not driven by Epstein Barr virus (EBV). Background T-cells show a follicular T helper cell (TFH) immunophenotype characterised by expression of CD57 and PD1. Therefore, the microenvironment of NLPHL differs in the typical and variant patterns [1, 9, 10].

In this study, we assessed the immunoarchitectural patterns of NLPHL as per the criteria given by Fan et al. and also evaluated the degree of variant patterns under the parameters set by Shet et al. [5, 8]. We also compared the growth patterns in biopsies of NLPHL patients at their initial diagnosis and relapse and evaluated their clinicopathologic characteristics. Through this study, an attempt has been made to emphasise on the importance of reporting the histological patterns of NLPHL and assess the prognostic implications of variant patterns.

Materials and methods

A retrospective histologic and immunohistochemistry (IHC) review of all archival slides of NLPHL over a period of 6 years from January 2015 to December 2020 was performed. Descriptive details about the clinical and follow-up information were obtained from the medical records department.

The histological and immunohistochemical findings of these cases were analysed. All cases were reviewed by two oncopathologists (N.M. and A.K. [senior pathologist]). Consensus diagnosis and scores were achieved by review and discussion at a multiheaded microscope. Additional IHC markers were performed on select cases as deemed necessary.

IHC was performed by immunoperoxidase staining on formalin-fixed paraffin-embedded tissue sections using the ultraView DAB Detection kit on the Ventana Benchmark XT platform. The antibodies used included CD3, CD4, CD5, CD7, CD8, CD10, CD15, CD20, CD21, CD23, CD30, CD45, CD68, CD79a, PAX5, OCT2, BOB1, PD-1, EMA, BCL6, BCL2, MUM1, ALK, LMP1, S100, and Ki-67. Identification of Epstein-Barr encoded ribonucleic acid (EBER) was done by in situ hybridisation (ISH).

All IHC staining patterns except PD-1 were assessed using a microscope viewed at P 4 \times , 10 \times , and 40 \times magnifications and were scored as positive, weakly positive (dim), or negative. Positivity in $> 50\%$ cells, when perceived at 4 \times magnification was labelled as strongly positive/positive. If positivity was better appreciated in $> 50\%$ of cells at any other magnification, the cells were labelled as weakly positive.

IHC for PD-1 was interpreted based on the intensity and number of TFH cells rosetting or ringing around LP

cells. The intensity was reported as bright if the PD-1-positive cells encircling LP cells were identifiable at 4× and 10× magnifications and dim if the PD-1 cells needed to be viewed at 40× magnification. The staining was reported as diffuse if > 50% LP cells were rosetted by PD-1-positive cells and focal if the number was < 50%.

Through this study, we aimed to classify the variant immunoarchitectural patterns of NLPHL as per Fan et al. [5]. We also scored the cases based on the histological parameters and tried to quantify the degree of variant pattern as per the scoring system described by Shet et al. (Table 1).

Results

(i) Patient characteristics

A total of 36 patients with NLPHL were included in our study. Of these, the descriptive details of clinical presentation and treatment were available in 25 cases. NLPHL constituted 6.4% of Hodgkin lymphoma cases in our institute.

The clinicopathologic features of these cases have been summarised in Table 2. Median age at diagnosis of NLPHL with variant histology was less as compared to that of patients with typical growth pattern (31 years

vs 42 years). A male predominance was noted with male/female ratio of 3.5:1. Nodal disease was seen in 35 cases. We also saw one case of primary extranodal NLPHL presenting as a soft tissue swelling in the right forearm in a 20-year-old male. Also, of the 25 cases for which clinical data was available, there were 15 (60%) cases which presented with an early-stage disease.

(ii) Morphologic spectrum

The immunoarchitectural patterns, scores, and complete LP cell immunophenotype for all patients are outlined in Table 3. The immunoarchitectural patterns were assigned by correlating histology with CD20 and CD3 IHC patterns. These patterns are enumerated in Fig. 1. Of the 36 biopsies, a total of 9 patients (25%) showed a predominant typical growth pattern, whereas 27 patients (75%) presented with variant histologies. The histologies mentioned in Table 2 include both pure and the major component seen in hybrid patterns. The frequencies of the individual immunoarchitectural patterns are summarised in Tables 3 and 4. Among patients with typical histology, the nodular pattern A was most commonly seen. On the other hand, pattern C with prominent extranodal LP cells was the most common variant pattern. The case with primary

Table 2 Clinicopathologic characteristics of NLPHL cases (including relapse cases)

	Typical histology (patterns A/B)		Variant histology (non-A/B patterns)	
Median age	42 years		31 years	
Number of cases	9/36 patients		27/36 patients	
Site	Nodal = 8	Extra nodal = 1	Nodal = 27	
Major immunoarchitectural patterns; Fan et al. (n = 36)	A = 6/9 B = 3/9		C = 15/27 D = 3/27	E = 7/27 F = 2/27
Average histological score out of 10; Shet et al. (n = 25)	~ 3 (2.89)		~ 6 (6.14)	
Clinical stage (n = 25)				
I/II	6		9	
III/IV	0		10	
Growth pattern at initial diagnosis (n = 25)	6		19	
Growth pattern at recurrence/relapse (n = 25)	0		7	
Average histological score out of 10 at recurrence/relapse; Shet et al. (n = 25)	NA		~ 8 (8.28)	
First-line treatment (n = 25)				
CT ± RT	3		2	
RT only	0		1	
Anti-CD20 antibody only	2		13	
Treatment unknown/refused	1		3	
Second-line treatment (relapsed; n = 7)				
Combination CT only	-		5	
High-dose CT + autologous stem cell transplant	-		2	

CT chemotherapy, NA not applicable, RT radiotherapy

Table 3 Immunophenotypic characteristics of neoplastic lymphocyte predominant cells and PD-1

Case	Biopsy type	Site	Pattern/s at diagnosis	Score	LCA	CD20	CD30	PAX5	Oct-2	Bob.1	BCL6	EMA	EBER	PD-1
1	EB	Axillary LN	Major=A Minor=B	3	P	P	P (subset)	P	P	P	P	N	N	Bright, diffuse
2	EB	Cervical LN	C	4	P	P	N	P	P	P	P	N	N	Bright, diffuse
3	EB	Inguinal LN	Major=E Minor=C	9	P	P	N	P	P	P	P	N	N	ND
4	EB	Inguinal LN	C	3	P	P	N	P	P	P	P	N	N	ND
5	EB	Axillary LN	C	5	P	P	N	P	P	P	P	P	N	ND
Relapse	EB	Cervical LN	Major=E Minor=C	9	P	P	N	P	P	P	P	N	N	ND
6	EB	SCLN	Major=E Minor=C	7	P	P	P (weak, subset)	P (dim)	P	P	P	N	N	ND
7	EB	Cervical LN	Major=E Minor=C	8	P	P	N	P	P	P	P	N	N	No rosettes
Relapse	EB	Inguinal LN	Major=E Minor=C	9	P	P	P (weak, subset)	P	P	P	P	N	N	No rosettes
8	EB	Axillary LN	Major=C Minor=B	2	P	P	N	P	P	P	P	N	N	Bright, diffuse
9	EB	Axillary LN	Major=E Minor=C	7	P	P	N	P	P	P	P	N	N	Dim, focal
10	EB	Interpectoral LN	Major=E Minor=C	8	P	P	P (subset)	P	P	P	P	N	N	Bright, focal
11	EB	Inguinal LN	Major=C Minor=E	8	P	P	N	P (dim)	P	P	P	N	N	Bright in 'C', dim in 'E'
12	EB	Inguinal LN	C	3	P	P	P (subset)	P	P	P	P	N	N	Bright, diffuse
13	EB	Periparotid LN	C	4	P	P	N	P	P	P	P	P	N	Bright, diffuse
14	EB	Cervical LN	F	6	P	P	P (subset)	P	P	P	P	N	N	Bright, diffuse
15	EB	Cervical LN	Major=D Minor=E	8	P	P	N	P	P	P	P	P	N	Dim, focal
Relapse	EB	Cervical LN	Major=E Minor=C	9	P	P	P (subset)	P	P	P	P	P	N	Dim, focal
16	EB	Inguinal LN	Major=C Minor=F	4	P	P	N	P	P	P	P	N	N	Bright in 'C', dim in 'F'
17	EB	Submandibular LN	Major=B Minor=F	5	P	P	N	P	P	P	P	N	N	ND
18	EB	Cervical LN	Major=C Minor=E	6	P	P	P (weak, subset)	P	P	P	P	P	N	Dim, focal
19	EB	Cervical LN	A	3	P	P	N	P	P	P	P	P	N	Bright, diffuse
20	EB	Axillary LN	Major=C Minor=B	4	P	P	P (subset)	P	P	P	P	P	N	Bright, diffuse
21	EB	Submandibular LN	A	1	P	P	P (subset)	P	P	P	P	N	N	Bright, diffuse

Table 3 (continued)

Case	Biopsy type	Site	Pattern/s at diagnosis	Score	LCA	CD20	CD30	PAX5	Oct-2	Bob.1	BCL6	EMA	EBER	PD-1
22	EB	Cervical LN	Major=E Minor=C	8	P	P	P (subset)	P	P	P	P	P	N	Dim, focal
Relapse	EB	Cervical LN	Major=F Minor=E	9	P	P	N	P	P	P	P	P	N	No rosettes
23	EB	Right arm swelling	Major=A Minor=B	3	P	P	N	P	P	P	P	N	N	Bright, diffuse
24	EB	Axillary LN	A	3	P	P	N	P	P	P	P	P	N	Bright, diffuse
25	EB	Periauricular LN	A	1	P	P	N	P	P	P	P	P	N	Bright, diffuse
26	EB	Cervical LN	Major=B Minor=C	3	P	P	N	P	P	P	P	N	N	Bright, diffuse
27	EB	Inguinal LN	F	7	P	P	P (subset)	P	P	P	P	N	N	Dim, focal
28	EB	Submandibular LN	C	6	P	P	N	P	P	P	P	P	N	Bright, diffuse
Relapse	EB	Posterior triangle LN	C	6	P	P	N	P	P	P	P	P	N	Bright, diffuse
29	EB	Inguinal LN	Major=E Minor=C	9	P	P	N	P	P	P	P	N	N	Dim, focal
30	EB	Postauricular LN	Major=B Minor=C	4	P	P	P (weak, subset)	P	P	P	P	N	N	Bright, diffuse
31	EB	External Iliac LN	D	9	P	P	N	P	P	P	P	N	N	Dim, focal
Relapse	EB	SCLN	D	9	P	P	N	P	P	P	P	N	N	Dim, focal
32	EB	Inguinal LN	Major=C Minor=E	7	P	P	N	P (dim)	P	P	P	N	N	Bright in 'C', dim in 'E'
33	EB	Inguinal LN	Major=C Minor=E	5	P	P	N	P	P	P	P	P	N	Bright in 'C', dim in 'E'
34	EB	Axillary LN	C	7	P	P	N	P	P	P	P	P	N	Dim, diffuse
Relapse	EB	Axillary LN	C	7	P	P	N	P (dim)	P	P	P	P	N	Dim, diffuse
35	EB	Cervical LN	C	4	P	P	N	P	P	P	P	P	N	Bright, diffuse
36	EB	Axillary LN	D	8	P	P	P (subset)	P	P	P	P	N	N	Dim, diffuse
Progression	CNB	Chest wall swelling	DLBCL											Negative

CNB core needle biopsy, DLBCL diffuse large B-cell lymphoma, EB excision biopsy, LN lymph node, N negative, ND not done, P positive, SCLN supraclavicular lymph node

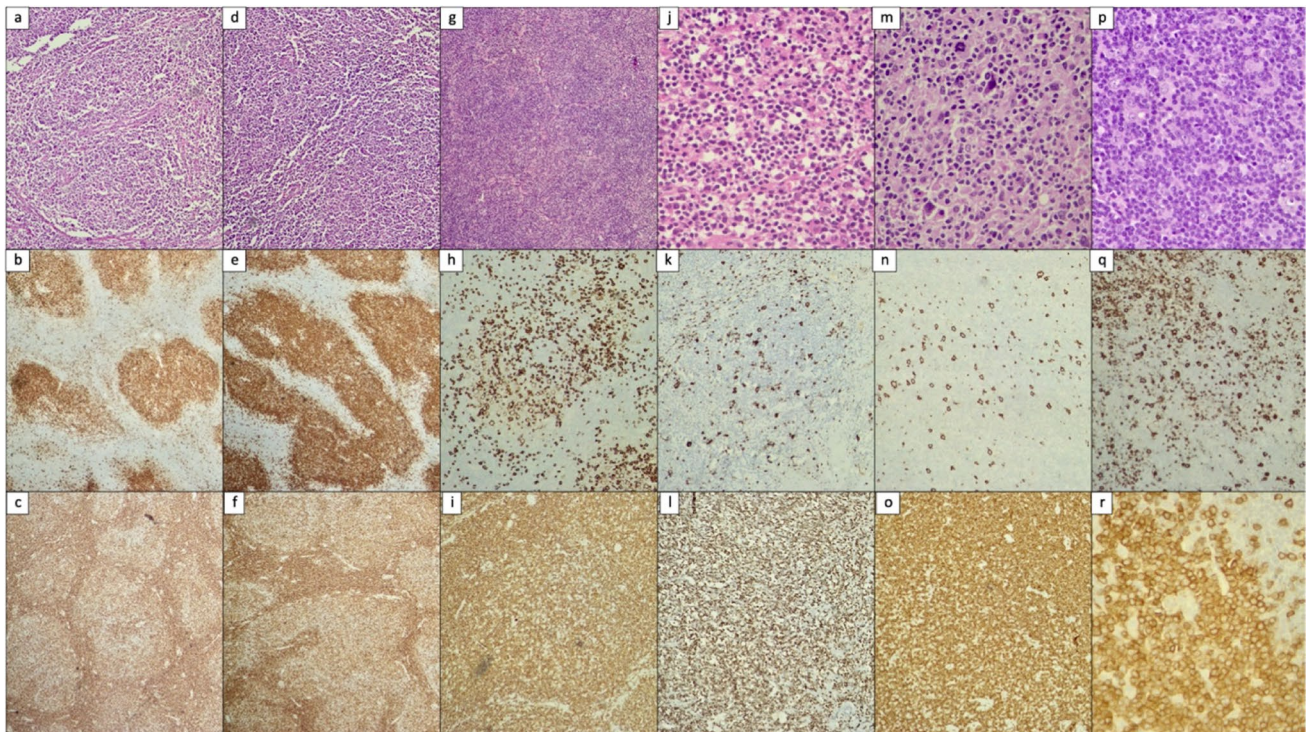


Fig. 1 **a** H&E 40× showing the classical nodular pattern A. The nodules are **b** B-cell-rich highlighted by immunohistochemistry for CD20 and show **c** internodular CD3 expression. **d** H&E 40× showing the typical serpiginous interconnected pattern B. The serpiginous interconnected nodules are B-cell-rich highlighted by **e** immunohistochemistry for CD20 and show **f** internodular CD3 expression. **g** H&E 40× showing the variant pattern C with prominent extranodular LP cells. The LP cells are highlighted by **h** immunohistochemistry for CD20 in a B-cell-rich background and show **i** intermixed CD3-positive

cells. **j** H&E 100× showing the variant T-cell-rich nodular pattern D. **k** The nodules show few LP cells highlighted by immunohistochemistry for CD20 and in a **l** CD3-positive T-cell-rich background. **m** H&E 100× showing the diffuse, T-cell-rich pattern E. Immunohistochemistry shows **n** few CD20-positive B-cells in a **o** diffuse, CD3-positive T-cell-rich background. **p** H&E 100× showing the diffuse, moth-eaten B-cell-rich pattern. Immunohistochemistry **q** for CD20 shows scattered LP cells and small lymphocytes with **r** intermixed CD3-positive T-cells

Table 4 Pattern-wise distribution of NLPHL cases

Immunoarchitectural patterns	Pure (n = 16)	Major/minor (n = 20)	Total
A Classic nodular	4	2 0	6
B Serpiginous/interconnected nodular	0	3 4	7
C Prominent extranodular LP cells	8	7 9	24
D T-cell-rich nodules	2	1 0	3
E Diffuse, T-cell-rich large B-cell-like	0	7 5	12
F Diffuse, mottled B-cell rich	2	0 2	4

extranodal presentation showed a major pattern A with a component of pattern B.

As seen in Tables 3 and 4 of the 36 biopsies with features of NLPHL, 16 (44.4%) showed a pure single pattern. None of these cases showed any a minor component of variant histology. A mixture of 2 patterns was noted in 20 (55.6%) cases. The various hybrid patterns observed in this study are enumerated in Table 5. The most common patterns of co-occurrence were C and E. None of the patients with pattern B histology occurred

Table 5 Patterns of co-occurrence in hybrid cases

Immunoarchitectural patterns	Total
Patterns C and E/E and C	11
Patterns B and C/C and B	4
Patterns A and B	2
Patterns D and E	1
Patterns B and F	1
Patterns C and F	1
Total	20

in a pure form in our study and most frequently showed an associated pattern C followed by pattern A.

As seen in Table 3, case number 36 from the study population underwent biopsies from two different sites and showed a simultaneous presentation of NLPHL with diffuse large B-cell lymphoma (DLBCL). While the biopsy from left supraclavicular lymph node showed histological features of NLPHL pattern D, biopsy from right chest wall swelling showed a dif-

ferent picture. This biopsy showed cohesive sheets of large atypical cells suggestive of a large B-cell lymphoma (LBCL) infiltrate of centroblastic type. This transformed DLBCL displayed a germinal centre B-cell (GCB)-type immunophenotype according to the Hans algorithm [11]. The LP cells in NLPHL displayed a CD20 + /CD10 – /BCL6 + /MUM1-positive immunophenotype. The large cells in DLBCL showed a similar immunoprofile to the LP cells seen in the supraclavicular lymph node and were CD10 – /BCL6 + /MUM1 –.

The typical cases with a nodular immunoarchitecture show expanded CD21 + and/ or CD23 + follicular dendritic cell (FDC) meshwork with many small B-cells, few histiocytes, and many PD1 + T-cell rosettes. On the other hand, cases with diffuse immunomorphologies showed an increase in histiocytes, decreased or absent B-cells, and fewer PD1 + T-cell rosettes.

The immune microenvironment in both typical and variant patterns showed a predominance of CD4 + T-cells. Expression of CD30 and EMA was noted in 12 (33.3%) and 13 (36.1%) out of 36 cases respectively. None of the cases showed CD15 expression. On relapse, 2 cases which were previously negative for CD30 showed dim expression in a subset of LP cells (Table 3). Association with EBV infection by LMP1 and EBER expression was not identified in any case.

(iii) Use of scoring system to identify variant patterns

The parameters enumerated by Shet et al. were scored by 2 pathologists by visual examination. The quantification was based on examination of H&E sections, CD20, CD3, CD21, and CD23 immunostains.

Cases with typical histologies were nodular throughout (7/9; 77.8%) or mostly nodular (2/9; 22.2%) with either well-defined, evenly distributed nodules seen on H&E (4/9; 44.5%) and irregular (3/9; 33.3%) or interconnected (2/9; 22.2%) nodules highlighted on CD20 immunostaining. Among the 27 cases with variant histologies, 6 cases (22.2%) were nodular throughout, all of which belonged to pattern C. The rest of the variant pattern C cases were mostly nodular (7/27; 25.9%) or showed < 75% nodularity (2/27; 7.4%). All cases with variant patterns D, E, and F (12/27; 44.5%) showed < 75% nodularity with irregular nodules which were highlighted on CD20 IHC.

Of the 16 cases with mixed histological patterns, 10 cases showed varying degrees of well defined to vague, irregular nodular areas intermixed with diffuse areas on H&E sections, CD20 and CD3 immunostains. The cases where nodular pattern was not well defined showed an increased number of CD3-positive T-cells. Among the 9 cases with typical histologies, 8 (88.9%) cases showed < 20% T-cell-rich area. More than 20%

T-cell-rich areas were seen in 25/27 cases (92.6%) with variant histologies.

All cases with typical histology showed completely preserved dendritic network on CD23 immunostaining (100%). Cases with variant histologies showed focally preserved dendritic network throughout the nodules (17/27; 63%) or loss of the network in most areas (10/27; 37%). T-cell-rich tumors ($\geq 50\%$ T-cell-rich areas) which showed loss of CD23 dendritic network constituted 9/27 (33%) cases with variant histologies.

Less than 15% extranodular LP cells were identified in 7 (77.8%) out of 9 cases with typical histologies. More than 15% extranodular LP cells were seen in 22/27 (81.5%) cases with variant histologies. The 5 cases with variant histologies which showed < 15% LP cells were all pattern C.

All cases with a typical growth pattern showed a score of ≤ 5 , while those with a variant histology showed a score between 2 and 9 (Table 3). Among the cases with variant histologies, 16 out of 27 cases (59.2%) showed a score of ≥ 6 . All cases with patterns D, E, and F showed scores of ≥ 6 .

(iv) Utility of PD-1 immunostaining

Results of IHC for PD-1 were available in 31 out of 36 cases (Table 3). PD-1 positivity was found in all NLPHL cases with typical A/B and mixed A/B histology (100%). Among the 23 cases with variant histologies, all 13 cases with pure and major pattern C histology showed PD-1-positive T-cells encircling the LP cells. Bright and diffuse PD-1 staining was noted in 11/13 (84.6%) cases with 1 case showing dim and diffuse and 1 case demonstrating dim, focal staining pattern. The staining pattern of PD-1 in the 3 pattern D cases was dim, focal in 2 cases (66.7%), and dim, focal in 1 case (33.3%). The 5 pattern E cases showed dim, focal PD-1 staining in 3 cases, bright focal staining in 1 case, and no staining in 1 case. Dim, focal PD-1 staining was seen in 1 case with pattern F.

Nodular and diffuse patterns in the same biopsies were identified in 9 cases. The nodular areas in all these biopsies were pattern C. The C/E variant was the most common histology constituting 8/9 cases followed by 1 case with patterns C/F. Among the C/E variant, the nodular areas showed bright PD-1-positive T-cells in 5/8 cases and dim in 3/8 cases. Dim and bright positive PD-1-positive T-cells encircling the LP cells in diffuse areas were noted in 5 and 1 cases respectively. One case showed no rosettes. Preserved, bright PD-1 immunostaining in the nodular areas was noted in 4 cases (44.4%) with diffuse areas showing a dim heterogenous intensity of staining for the same (Fig. 2).

Therefore, even though PD-1 reactivity was conserved in the nodular areas in 8/9 cases (88.9%), in

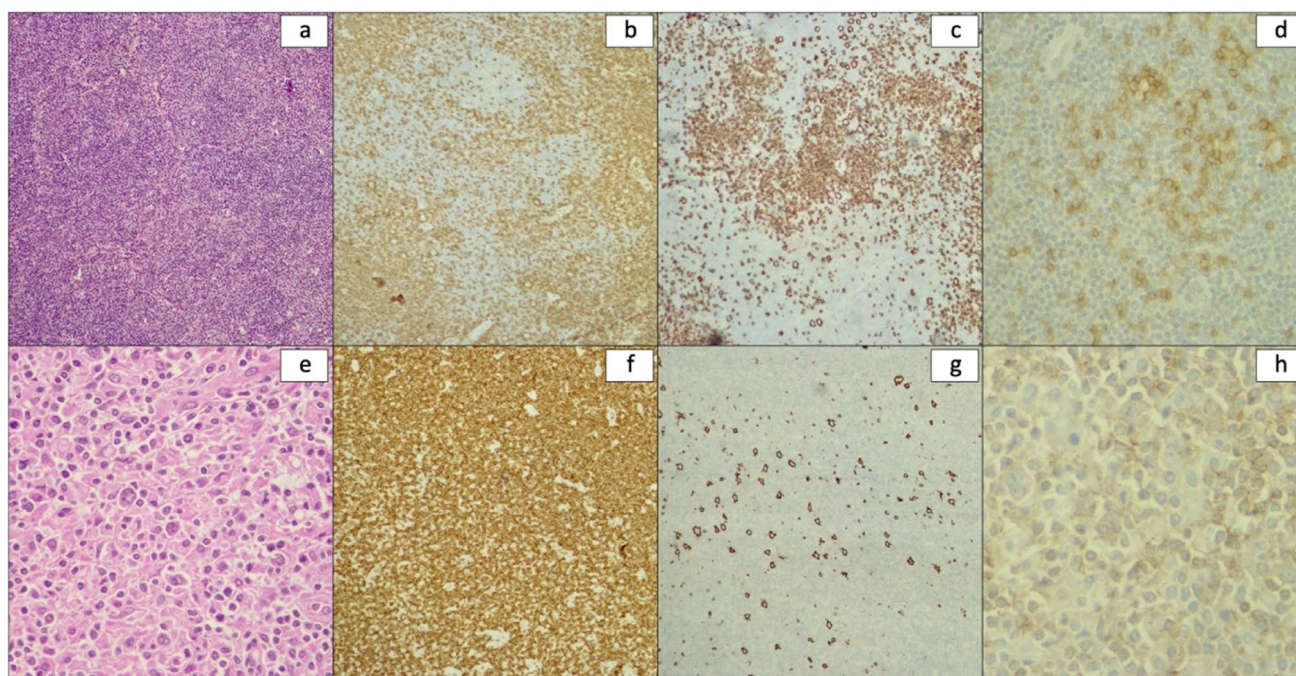


Fig. 2 **a** H&E 10× showing the variant pattern C. **b** CD3-positive internodular cells with **c** B-cell-rich nodules showing prominent extranodal LP cells. **d** The LP cells are rosetted by PD-1-positive T-cells. The intensity of staining is bright. Same biopsy showed **e**

T-cell-rich areas with pattern E where the **f** background T-cells were diffusely positive for CD3 with **g** singly scattered CD20-positive LP cells. **h** The LP cells are rosetted by dimly stained T-cells

these cases, the diffuse component also showed variable retention of PD-1 reactivity in 5/9 cases (55.6%).

Of the 7 cases which relapsed, immunoreactivity results of PD-1 could be retrieved in 6 cases. One case was negative for PD-1 immunostaining at initial diagnosis and relapse. When first detected, dim focal, bright diffuse, and dim diffuse staining patterns of PD-1 were noted in 3, 1, and 1 cases respectively. At relapse, only one case showed a change in staining pattern from dim focal to no staining.

(v) *Relapse and treatment characteristics*

Of the 25 cases for which clinical data was available, relapse of lymphoma was seen in 7 cases (28%), all of which showed variant histology on initial diagnosis (Table 2). The median time to lymphoma recurrence ranged from 4 months to 11 years with a median of 1 year. The histological patterns and scores at initial diagnosis and relapse are summarised in Table 2.

The histopathological growth patterns at initial diagnosis and relapse were concordant in 4 out of 7 cases (Table 3). Histopathological scores increased or remained the same. All 7 cases of recurrence showed > 50% T-cell-rich areas, and 6/7 cases showed > 50% extranodal LP cells. Table 2 also sum-

marises the patient pathological and treatment characteristics of relapsed NLPHL cases.

Discussion

This study presents the clinical and pathologic features of NLPHL, assesses the frequency of relapse, and studies the prognostic implications of different histopathological growth patterns at the time of initial biopsy and relapse.

NLPHL shows male preponderance with middle-aged men accounting for 75% of cases [1, 12]. In the present study, a male preponderance was noted with a median age of 32 years. The median age at diagnosis of NLPHL with variant histologies was much less as compared to patients with typical histology (30 years vs. 42 years). This is different from the results given by Hartmann et al. who stated that the median ages between the two histologic groups were comparable in their study [7].

Primary extranodal presentation of NLPHL is exceedingly rare with only 7 cases reported in literature [4, 13–18]. Involvement of extranodal sites at initial presentation with simultaneous nodal disease has been noted in 6% cases which are mostly synchronous with nodal disease

[4]. The case encountered by us was unique in its presentation. This 20-year-old male patient presented with a long duration of subcutaneous swelling in both forearms which were gradually increasing in size. While the left arm swelling was diagnosed as schwannoma, the right arm swelling showed characteristic morphologic and immunophenotypic features of NLPHL despite the unusual anatomic site. To our knowledge, this is the first case of extranodal NLPHL primarily involving the soft tissue.

Unveiling the diagnosis of NLPHL which presents primarily as an extranodal disease poses diagnostic challenges. Unexpected sites of presentation should not preclude a diagnosis of NLPHL if sufficient morphologic, immunohistochemical and clinical criteria are fulfilled.

Secondary transformation to diffuse large B-cell lymphoma (DLBCL) concurrently or subsequent to the diagnosis of NLPHL is seen in 20–30% of cases [10, 19]. In our case, while the tumor microenvironment in pattern D NLPHL showed a predominance of small T-lymphocytes, the DLBCL component showed a variable proportion of admixed histiocytes. Also, even though the immunophenotype of LP cells and large B-cells was similar, an up-regulation of BCL2 protein in DLBCL was identified. This was similar to the findings reported by Hartmann et al. who observed that the up-regulation of anti-apoptotic BCL2 enhanced the survival properties of ‘LP-type’ tumor cells in DLBCL [19].

Histopathologically, 26.5% patients in our study showed a pure/predominant typical NLPHL infiltrate, and 73.5% cases were labelled as NLPHL variants. Similar to our work, the studies by Fan et al. and Shet et al. [5, 8] also showed more frequent variant patterns in contrast to the studies by Hartmann et al. where predominant typical histomorphology was seen in 74.6% and 52.7% cases respectively [3, 7]. It is likely that these data do not reflect the true frequencies of typical and variant NLPHL patterns in our population because only a subset of patients are referred to a tertiary cancer centre for treatment. Studies on larger sample size are needed to determine the exact rate of typical and variant morphologies of NLPHL.

In the present analysis, of the 19 cases with variant NLPHL histology, 7 relapsed. A limitation of our study is the lack of clinical details in nearly one-third of the cases. Among the cases for which data was available, none with typical NLPHL infiltrate showed disease progression/relapse. All patients that relapsed showed a histopathological score between 6 and 9. Concordance of histopathological growth patterns during the initial diagnosis and relapse was seen in more than half of the patients who relapsed in our study, similar to the study by Hartmann et al. done in 2019. The study by Hartmann et al. showed variant histology to be an independent prognostic factor for disease progression/relapse [7]. Our findings also corroborated the cut-off level set by Shet et al. who said that a cut-off score of 6 can be used as an objective guide to distinguish typical from variant patterns [8].

Tumor microenvironment has been known to play a role in the development and progression of NLPHL [3, 20]. Bien et al.

have identified an immunological synapse between the LP cells and the surrounding TFH cells and state that NLPHL occurs due to the interaction between LP cells and the rosetting T-cells with a TFH phenotype. A gradual decrease in the intensity of PD-1 staining from nodular to diffuse areas was noted in 44.4% (4/9) cases. However, this finding was not specific as 55.6% (5/9) cases also showed variably intense PD-1 immunostaining in the diffuse areas. Also, among the cases which relapsed or progressed, only two cases showed a change in the PD-1 staining intensity. Therefore, even though there was a relative loss of PD-1 expression in diffuse areas, whether this finding indicates a potential for disease progression warrants further investigation on a larger sample size. This finding was akin to the study by Churchill et al. who observed a high number of PD-1-positive T-cells in areas with diffuse morphology. Moreover, rings of PD1-positive T-cells are also seen in classical Hodgkin lymphoma, in T-cell histiocyte-rich large B-cell lymphoma, and in reactive viral infections making this a relatively non-specific feature for the diagnosis of NLPHL [9, 20].

On quantification of tumor microenvironment by CD3 and CD20 immunostains, we noted a limited number of atypical large B-cells, i.e., LP cells with variable small T- and B-lymphocytes in the microenvironment. A T-cell-rich microenvironment with varying degrees of nodular or diffuse patterns has been associated with a higher clinical stage [3, 7, 8]. Higher clinical stage was seen in 40% cases (10/25 cases) with variable histologies in this study, all of which showed > 20% T-cells in the background. Hartmann et al. have attributed the alterations in the microenvironment to be associated with dissemination of LP cells to distant lymph nodes [7].

To summarise, this study documents the typical and variant morphologic patterns of NLPHL and supports the utility of the scoring system given by Shet et al. Results of present study also state that tumors with variant histopathology and scores > 6 showed an increased risk of relapse. Our findings show consistency of histopathological growth patterns at initial diagnosis and relapse. This study also suggests that decrease/increase in intensity of PD-1 immunostaining may not necessarily point towards the presence of a diffuse architecture or disease progression. Therefore, in this era of molecular diagnostics, this data emphasises on the necessity of correlating histomorphology and IHC findings in the diagnosis of NLPHL.

Declarations

Ethics statement Ethics Committee approval has been obtained via Institutional Ethics Committee, Apollo Hospitals.

Patient consent statement Not applicable. This is an observational study. This study does not involve any risk to the patient. Patient consent was not available; no personal details which may identify the patient are included in this submission.

Conflict of interest The authors declare no competing interests.

References

1. Swerdlow SH, Campo E, Harris NL et al (2017) WHO classification of tumours of haematopoietic and lymphoid tissues. International Agency for Research on Cancer, Lyon, pp 424–434
2. Savage KJ, Skinnider B, Al-Mansour M et al (2011) Treating limited-stage nodular lymphocyte predominant Hodgkin lymphoma similarly to classical Hodgkin lymphoma with ABVD may improve outcome. *Blood* 118:4585–4590. <https://doi.org/10.1182/blood-2011-07-365932>
3. Hartmann S, Eichenauer D, Plütschow A, Mottok A, Bob R, Koch K et al (2013) The prognostic impact of variant histology in nodular lymphocyte-predominant Hodgkin lymphoma: a report from the German Hodgkin Study Group (GHSG). *Blood* 122(26):4246–4252. <https://doi.org/10.1182/blood-2013-07-515825>
4. Rangan A, Grahn S, Feldman A (2017) Nodular lymphocyte predominant hodgkin lymphoma of the ileum. *Case Reports Pathol* 2017:1–4. <https://doi.org/10.1155/2017/5981013>
5. Fan Z, Natkunam Y, Bair E, Tibshirani R, Warnke R (2003) Characterization of variant patterns of nodular lymphocyte predominant hodgkin lymphoma with immunohistologic and clinical correlation. *Am J Surg Pathol* 27(10):1346–1356. <https://doi.org/10.1097/00000478-200310000-00007>
6. Gloghini A, Bosco A, Ponzoni M, Spina M, Carbone A (2014) Immunoarchitectural patterns in nodular lymphocyte predominant Hodgkin lymphoma: pathologic and clinical implications. *Expert Rev Hematol* 8(2):217–223. <https://doi.org/10.1586/17474086.2015.991388>
7. Hartmann S, Plütschow A, Mottok A, Bernd H, Feller A, Ott G et al (2019) The time to relapse correlates with the histopathological growth pattern in nodular lymphocyte predominant Hodgkin lymphoma. *Am J Hematol* 94(11):1208–1213. <https://doi.org/10.1002/ajh.25607>
8. Shet T, Panjwani P, Epari S, Sengar M, Prasad M, Arora B et al (2014) A simplified scoring system to document variant patterns in nodular lymphocyte predominant Hodgkin lymphoma. *Leuk Lymphoma* 56(6):1651–1658. <https://doi.org/10.3109/10428194.2014.961013>
9. Churchill H, Roncador G, Warnke R, Natkunam Y (2010) Programmed death 1 expression in variant immunoarchitectural patterns of nodular lymphocyte predominant Hodgkin lymphoma: comparison with CD57 and lymphomas in the differential diagnosis. *Hum Pathol* 41(12):1726–1734. <https://doi.org/10.1016/j.humpath.2010.05.010>
10. Younes S, Rojansky R, Menke J, Gratzinger D, Natkunam Y (2021) Pitfalls in the diagnosis of nodular lymphocyte predominant hodgkin lymphoma: variant patterns, borderlines and mimics. *Cancers* 13(12):3021. <https://doi.org/10.3390/cancers13123021>
11. Hans CP, Weisenburger DD, Greiner TC et al (2004) Confirmation of the molecular classification of diffuse large B-cell lymphoma by immunohistochemistry using a tissue microarray. *Blood* 103:275–282. <https://doi.org/10.1182/blood-2003-05-1545>
12. Anagnostopoulos I, Hansmann ML, Franssila K, Harris M, Harris NL, Jaffe ES, Han J, Van Krieken JM, Poppema S, Marafioti T, Franklin J, Sextro M, Diehl V, Stein H (2000) European Task Force on Lymphoma project on lymphocyte predominance Hodgkin disease: histologic and immunohistologic analysis of submitted cases reveals 2 types of Hodgkin disease with a nodular growth pattern and abundant lymphocytes. *Blood* 96(5):1889–1899. <https://doi.org/10.1182/blood.V96.5.1889>
13. Williams T, Raess P, Brazier R, Cascio M (2019) Primary extranodal nodular lymphocyte predominant Hodgkin lymphoma involving the thyroid. *Head Neck Pathol* 14(2):550–553. <https://doi.org/10.1007/s12105-019-01052-y>
14. Yencha MW (2002) Primary parotid gland Hodgkin's lymphoma. *Ann OtolRhinolLaryngol* 111:338–342. <https://doi.org/10.1177/000348940211100410>
15. Parikh JG, Bilal M, Tombazzi C et al (2014) A rare case of primary pancreatic Hodgkin lymphoma. *J Gastrointest Cancer* 45(Suppl 1):10–13. <https://doi.org/10.1007/s12029-013-9521-7>
16. Ali H, Naresh K, Aqel NM (2013) Primary nodular lymphocyte predominant Hodgkin lymphoma of the palate: a rare incidence which was also associated with progressive transformation of germinal centres of cervical lymph node. *J Egypt Natl Cancer Inst* 25:161–163. <https://doi.org/10.1016/j.jnci.2013.04.001>
17. Bohn-Sarmiento U, Rivero-Vera JC, Aguiar-Bujanda D et al (2006) Primary Hodgkin's lymphoma of the caecum. *Clin Transl Oncol* 8:450–452. <https://doi.org/10.1007/s12094-006-0200-z>
18. Li WS, Wang RC, Wang J et al (2015) Primary nodular lymphocyte-predominant Hodgkin lymphoma of uterine cervix mimicking leiomyoma. *Clin Case Rep* 3:349–352. <https://doi.org/10.1002/ccr3.246>
19. Hartmann S, Eray M, Döring C, Lehtinen T, Brunnberg U, Kujala P et al (2014) Diffuse large B cell lymphoma derived from nodular lymphocyte predominant Hodgkin lymphoma presents with variable histopathology. *BMC Cancer* 14(1):332. <https://doi.org/10.1186/1471-2407-14-332>
20. Bein J, Thurner L, Hansmann M, Hartmann S (2020) Lymphocyte predominant cells of nodular lymphocyte predominant Hodgkin lymphoma interact with rosetting T cells in an immunological synapse. *Am J Hematol* 95(12):1495–1502. <https://doi.org/10.1002/ajh.25972>

Publisher's note Springer Nature remains neutral with regard to jurisdictional claims in published maps and institutional affiliations.

Springer Nature or its licensor holds exclusive rights to this article under a publishing agreement with the author(s) or other rightsholder(s); author self-archiving of the accepted manuscript version of this article is solely governed by the terms of such publishing agreement and applicable law.